

Directed percolation criticality due to stochastic switching between attractive and repulsive coupling in coupled circle maps

Abhijeet R. Sonawane

Centre for Modeling and Simulation, University of Pune, Pune 411 007, India

(Received 18 November 2009; revised manuscript received 22 February 2010; published 18 May 2010)

We study a lattice model where the coupling stochastically switches between repulsive (subtractive) and attractive (additive) at each site with probability p at every time instant. We observe that such a kind of coupling stabilizes the local fixed point of a circle map, with the resultant globally stable attractor providing a unique absorbing state. Interestingly, a continuous phase transition is observed from the absorbing state to spatiotemporal chaos via spatiotemporal intermittency for a range of values of p . It is interesting to note that the transition falls in class of directed percolation. Static and spreading exponents along with relevant scaling laws are found to be obeyed confirming the directed percolation universality class in spatiotemporal intermittency regime.

DOI: [10.1103/PhysRevE.81.056206](https://doi.org/10.1103/PhysRevE.81.056206)

PACS number(s): 05.45.Ra, 47.27.Cn, 64.60.Ht

I. INTRODUCTION

Considerable progress has been made in the study of non-equilibrium statistical processes for a set of diversified systems in last few decades. In such systems, the temporal evolution starts far from equilibrium initial conditions. The relaxation to some stationary state essentially depends on probabilistic local dynamics due to the absence of coarse-grained free energy or Lyapunov potential, which is attributed to the evolution involving irreversibility, since the condition of detailed balance is not satisfied in these systems. Time plays the role of an additional degree of freedom in such systems. Consequently, there is no obvious symmetry between spatial and temporal degrees of freedom, which results in a rich variety of phases and patterns that can be observed in different parameter regimes. The general theoretical starting point is a set of deterministic equations with stochastic modifications or additions if necessary, e.g., master equations, Langevin equations, partial differential equations, mean-field rate equations, etc. These approaches have been applied in variety of systems such as the Ising model [1], catalytic process [2], etc. The dynamics of creation of pattern generally involves linear instabilities due to parameter inhomogeneities, symmetry breaking, defects, etc. Sometimes these nonequilibrium systems involve transitions between different dynamical phases with a tunable parameter. The usual concepts of equilibrium statistical mechanics such as *universality* and *critical phenomena* can be applied to such nonequilibrium systems as well. Indeed, the universality classes and scaling laws will be diverse and characteristically different from their equilibrium counterparts due to various symmetries and significance of local dynamics. In Ref. [3], an excellent review of different systems in this regard is presented. Such systems do not obey usual equilibrium statistical laws, which renders them analytically less tractable except a few notable cases as one-dimensional reaction-diffusion process, symmetric exclusion process, etc. Exact methods of many-body quantum physics and noncommuting algebra have been gainfully applied in exactly solving some of the nonequilibrium processes. However, a large class of such nonequilibrium processes still awaits exact ana-

lytical solutions. One such, easy to define, process with very nontrivial critical behavior is the universality class of *directed percolation (DP)*.

In the last two decades there has been considerable focus on various systems showing DP behavior and investigating the routes to DP behavior by means of master equations, reaction-diffusion processes, Monte Carlo Simulations, and various approximation techniques [4]. Various models such as pair contact process, threshold transfer process, asymmetric exclusion process, phenomenological reaction-diffusion systems, and there variants have been used to explain DP behavior and to obtain the pertinent critical exponents. Absorbing phase transitions, such as synchronization [5], epidemic spreading [4], wetting [6], self-organized criticality [7], and several other experimental studies [8] fall under DP universality class. The debate about “naturalness” of synchronous and asynchronous updating rules has also been pursued while studying DP universality class model systems. Critical phenomenon on complex networks has also been extensively studied [9]. DP class has been mainly identified with spreading process which is described as a competition in infection and recovery.

Studies on several lattice models such as Domany-Kinzel cellular automata and contact processes have been very helpful in understanding DP as a process of the interacting particles. The general reaction-diffusion scheme corresponding to spreading in DP process involves self-annihilation, diffusion, offspring production, and coagulation of the particles [4]. The competition between these processes gives rise to spreading phenomena and pattern formation in space and in time. Many variants of these processes have been studied and found to be falling in DP class. Some of them actually have given rise to new universality classes in nonequilibrium phase transitions [3] due to new symmetries, disorders, and fluctuations. In general, systems under DP class can be said to have followed the dynamics of competition between varieties of aforementioned processes.

Deterministic systems such as coupled map lattice (CML) have been toy models for studies in pattern formation and spatially extended systems. These systems provide great deal of numerical simplicity along with being analytically solv-

able. Transition to synchronization and spatiotemporal intermittency (STI) route to spatiotemporal chaos has been well studied in these systems. Chate and Manneville introduced a simple CML [10] exhibiting spatiotemporal intermittency and found that the onset of spatiotemporal intermittency did not fall in DP class. This apparent nonuniversality was attributed to the traveling solitons with comparatively longer lifetimes [11]. This discrepancy was removed by Rolf *et al.* [12] by using an asynchronous updating rule. The asynchronous updating rule prevented various spatiotemporal structures from forming which may introduce long-range correlations which destroy DP. Later, Janaki *et al.* [13] showed that the onset of spatiotemporal intermittency in deterministic system of coupled circle maps is in DP universality class. Local persistence exponent for this system further validated the argument [14]. This system is quite distinct from the system suggested by Chate and Manneville [10] and provided due credence to the Pomeau conjecture [15]. It is worthwhile to mention that it is nontrivial to map deterministic dynamics to stochastic behavior. The system provides a laboratory to test the validity of DP class. The full phase space of coupled circle map was explored and classified by Jabeen and Gupte [16]. Studies on decay distributions of laminar domains in rheology of nematogenic fluids further showed that the onset of spatiotemporal intermittency is indeed a DP universality class testbed [17].

Many studies suggest connection between spatiotemporal intermittency and DP processes from point of view of numerical estimation of critical exponents. As mentioned above, the competition between various processes such as offspring production, coagulation, and self-destruction leads to DP behavior. It is then imperative to ask: can these processes be mimicked by analogous behaviors in CML models bearing in mind the robustness of DP universality transition? In this paper, we try to answer this question in the affirmation by actually finding such a system and exploring its spatiotemporal behavior. In Sec. II we introduce the model of stochastically switched coupling in CMLs. Section III comprises results regarding stabilization properties of the model and numerical estimation of critical exponents. In Sec. IV, a set of dynamic exponents is obtained and transition of DP universality class is shown. In Sec. V, we conclude our findings.

II. STOCHASTICALLY COUPLED MAPS

We are interested in mainly simulating the mechanism in DP processes using tools of coupled circle maps which have been extensively studied in last few years. Mainly, coupled circle maps are studied using positive (i.e., attractive) diffusive coupling. Various spatiotemporal structures were mentioned in the phase diagram obtained in [16]. Recent results about the nonuniversal dependence of spatiotemporal regularity in randomly coupled circle map lattice add importance to nodal dynamics [18]. In CML, the coupling tends to make the system homogeneous and the local dynamics add temporal inhomogeneity. Repulsively coupled systems have been investigated from the point of view of synchronization [19] and nonlinear dynamics in cardiac myocytes [20]. The un-

stable type of coupling was also studied by Neufeld and Vicsek [21]. It has also been found that the ecological webs typically have both positive and negative connections between the components [22]. The couplings between neurons have been found to be both excitatory and inhibitory [23]. Recently, Chen *et al.* [24] investigated the phase diagram from positive and negative couplings in Lorenz system. The system displayed various phenomena as synchronization (in phase and antiphase) and amplitude death. Coupled circle maps with negative coupling investigated by Gade *et al.* [25] showed region of traveling waves characterized by algebraic decay of persistence. This behavior was explained using cellular automata model and Motzkin paths. This kind of repulsive coupling in regular CML leads to subtractive interaction of local site with its nearest neighbors as opposed to additive interaction in positive coupled map lattices. We conjecture that the repulsive interaction due to subtractive coupling can be emulated as an offspring production process in DP where nearest neighbor infects the local site due to negative Laplacian facilitating the propagation of perturbations. On the contrary, the positive coupling can be considered as a version of coagulation or annihilation process. In fact, self-destruction can be merely accounted for as a local site going to a fixed point. The DP models involve critical percolation probability which marks the phase transition. In order to have such a stochastic element in our model, we introduce coupling probability as explained below. We introduce the model as follows. We interpolate between two extremes of repulsive [25] and attractive [13] couplings.

We assign a continuous variable $x_i(t)$ at each site i at time t , where $1 \leq i \leq L$ with L as the system size. The evolution of $x_i(t)$ is defined by

$$x_i(t+1) = \begin{cases} f(x_i(t)) - \frac{\epsilon}{2}[x_{i-1}(t) + x_{i+1}(t) - 2x_i(t)], & \text{if } \eta < p \\ f(x_i(t)) + \frac{\epsilon}{2}[x_{i-1}(t) + x_{i+1}(t) - 2x_i(t)], & \text{otherwise.} \end{cases} \quad (1)$$

The parameter ϵ is the coupling strength, $0 < \eta < 1$ is a uniformly distributed random number picked for each site at each time. p is the coupling probability deciding the time-dependent switching between attractive and repulsive couplings. The local dynamical update function $f(x)$ is the circle map, $f(x) = x + \omega - \frac{k}{2\pi} \sin(2\pi x)$. We confine the dynamics to the interval $[0,1]$ using the following rule. If $\text{int}[x_i(t)] = m$, $x_i(t) = x_i(t) - m$ if $x_i(t) > 0$ and $x_i(t) = x_i(t) - m + 1$ if $x_i(t) < 0$. The coupling probability p takes values in the interval $[0,1]$, where $p=0$ pertains to positively coupled map lattice and $p=1$ corresponds to dynamics studied by Gade *et al.* [25] with negative coupling. Notice that, we use linear form of coupling. We fix the value of $\omega=0.068$ and $k=1$. The fixed point solution for the local map $f(x)$ is given by

$$x^* = \frac{1}{2\pi} \sin^{-1} \left(\frac{2\pi\omega}{k} \right). \quad (2)$$

We can define the dynamics at site i to be laminar if $|x_i(t) - x^*| < \delta$ for a small enough $\delta \sim 0.0001$ and to be turbulent, otherwise.

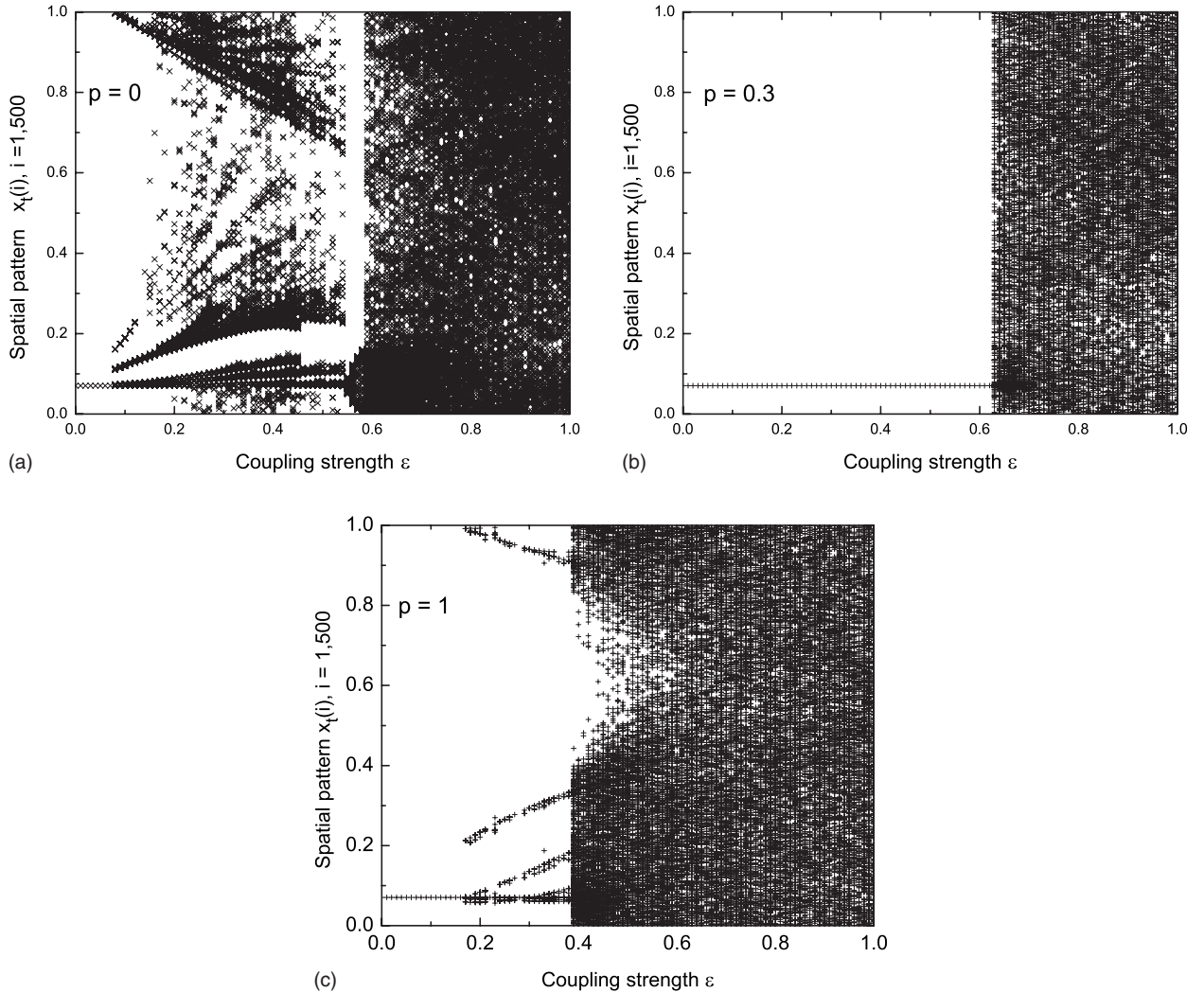


FIG. 1. Bifurcation diagram with spatial pattern, at an instant of time (after transience), with respect to coupling strength ϵ for $L=500$ (sites) for three different p values. (a) $p=0$, shows all the spatial structures in positive coupled circle map lattice for $\omega=0.068$. (b) $p=0.3$, this corresponds to attractor widening crisis route to STI marking the DP transition point at $\epsilon_c=0.627$. (c) $p=1.0$, bifurcation diagram for repulsively coupled map lattice where the turbulent spots move like traveling waves; this feature is seen for $0.155 \leq \epsilon \leq 0.36$ [25].

III. RESULTS AND DISCUSSION

A. Stabilization of steady state

Coupled motile oscillators have been modeled with time-dependent interaction which switches alternately from inhibitory to excitatory, depending on the status of an internal variable, and this leads to formation of clusters [26]. Introduction of statistical coupling has important bearing on the stability properties of our system. We present some results which show that the state $x(i)=x(j)=x^* \forall i,j,t$ gains stability for adequate coupling strength in the presence of time-dependent switching of coupling, with x^* being the nontrivial fixed point. The creation of windows of stability happens to take place for all finite values of p , which means that small fraction of negative links, in an otherwise positively coupled circle map, facilitates in the local fixed point becoming a global attractor. This type of spatiotemporal synchronization in coupled maps has been achieved by various means such as introducing random nonlocal connectivity [27,28]. Rapid

switching of random links also stabilizes the fixed point [29]. Numerous studies of time delayed coupling in variety of systems, including CMLs [30], have shown the way of achieving such synchronization. Recent studies also incorporated effects of random delays of various distributions and network topologies and showed the existence of windows of stability which are otherwise absent in uncoupled maps [31]. Here, in this system we show that such a kind of synchronization can be obtained in coupled circle maps when we allow the coupling to switch between attractive and repulsive.

Turova [32] showed that an inhibitory neuron incorporated into a population of connected excitatory neurons stabilized the oscillations of total activity. In our case the fraction of negatively coupled sites in the network can be determined by coupling probability p . In this sense, the parameter p can be considered as balance between repulsive and attractive coupling links in the network.

It can be seen from the spatial bifurcation pattern shown in Fig. 1(b) for $p=0.3$ that the fixed point becomes a *stable global attractor* in the range $0 < \epsilon < \epsilon_c$. In Fig. 1(a), the bi-

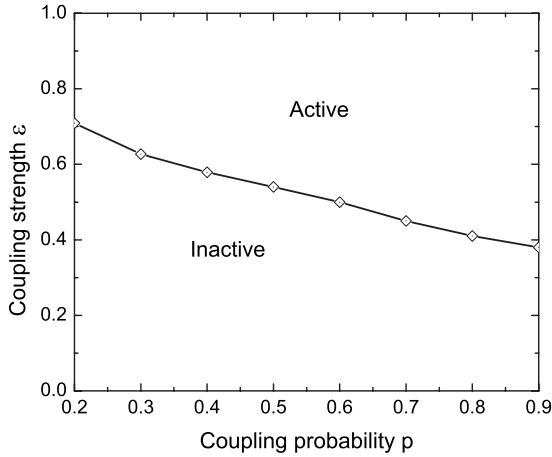


FIG. 2. Schematic phase diagram in ϵ - p plane. Critical edge between laminar (inactive) and turbulent (active) sites where DP transition occurs for $L=1000$.

furcation diagram for $p=0$, i.e., all couplings are positive, is depicted, and in Fig. 1(c) the same for $p=1$ (all repulsive) is shown. The value of ϵ_c changes monotonically with respect to p as can be inferred from the phase diagram in Fig. 2. At the extremes i.e., in the cases of $p=0$ and 1, we have all attractive CML and all repulsive coupling considered by Gade *et al.* [25]; here, we have interpolated between these two extreme regimes. At each instant of time, each site chooses among the two coupling types: positive or negative. There is a clear transition where the global attractor loses stability and the system transits to spatiotemporal chaos. Such a transition from synchronized state to incoherent state can be characterized by average error function defined as

$$Z = \left\langle \frac{1}{L} \sum_{i=1}^L [x_i(t) - \bar{x}]^2 \right\rangle_t, \quad (3)$$

where $\langle \dots \rangle_t$ denotes temporal average and \bar{x} is the average over elements of an array $[1/L \sum_{i=1}^L x_i(t)]$.

Figure 3 displays the average error Z vs ϵ for various values of p . It may be observed that for large range of ϵ there is in-phase synchronization among the elements of the lattice. The value of p is increased from $p=0.2$ to 0.9 with each curve as we move from right to left. The stabilization is observed even for small values of p . As reported in the earlier works, in achieving stabilization, array architecture, feedback, and delay played a role. Here, synchronization is achieved in an otherwise unstable lattice by changing the nature of coupling statistically in a fixed neighborhood. The spatiotemporal structure is evident from density plots shown in Fig. 4. We fix the value of $p=0.3$ and show plots for different values of ϵ pertaining to different dynamical regimes. Site index is plotted along the x axis and time evolves about the y axis. For $\epsilon=0.5$ shown in Fig. 4(a), the final state is a stabilized fixed point or all laminar state. Upon further increase in coupling strength to $\epsilon=0.7$ in Fig. 4(c), the system displays a fully developed spatiotemporal chaos. In the intermediate value of coupling strength another interesting phenomenon occurs. At $\epsilon=0.627$ shown in Fig. 4(b) turbu-

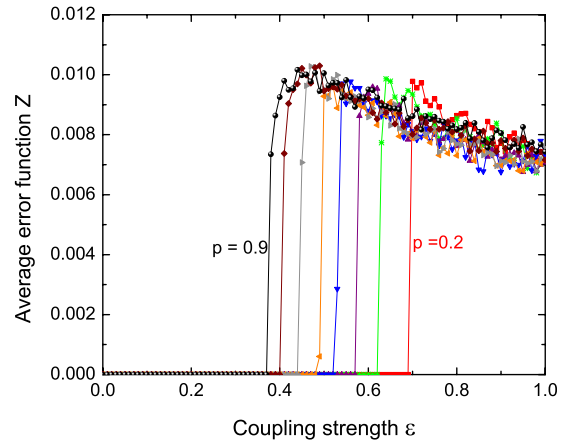


FIG. 3. (Color online) Average error function plotted against coupling strength with increasing value of p from right $p=0.2$ to left $p=0.9$. We can see the range of fixed point decreasing with increasing p . These are also the point where DP transition occurs.

lent clusters start to appear and give rise to spatiotemporal intermittency. In this state, a site can become turbulent or laminar. The spatiotemporal intermittency arises due to attractor widening crisis. Due to this sudden crisis the globally fixed point loses stability and the variable $x(i)$ can now traverse the entire phase space. Sudden bursts of turbulent activity occur in the system, and this marks a dynamical phase transition from laminar to chaotic regimes which we will characterize in the next section.

B. Dynamic phase transition in DP class

In the previous section we have seen that the system undergoes a phase transition from a fixed point state to a chaotic state. In CML, the laminar site can turn into turbulent site only if at least one of its neighbors was turbulent at previous time. On the contrary, a turbulent site might be driven to a fixed point by its laminar neighbors. This might depend on the type of local interaction that takes place among neighboring sites. The subtractive interaction might induce turbulence and additive interaction might drive the site toward a fixed point. This can be understood from the fact that positive coupling will move the turbulent site with laminar neighbors to a fixed point. For example, if $x(i) > x^*$, positive coupling will lower the value of $x(i)$ moving it closer to the fixed point; the opposite will happen if $x(i) < x^*$, where the value will be raised toward the fixed point. On the contrary, the repulsive coupling will enhance the growth of small wavelength spatial disturbances even if a local map tends toward stable conditions arising due to positive coupling. The local onsite chaotic dynamics indeed allows the site to go to a fixed point and become laminar once it is in the basin of attraction of a fixed point. It can be seen that such a kind of transition appears clearly due to the type of stochastic coupling applied here. Now, we can consider these processes to be analogous with particle creation, pair annihilation, and self-destruction process in DP universality class. In DP, the bond can be either open or closed depending on probability; the stochastic coupling probability here in-

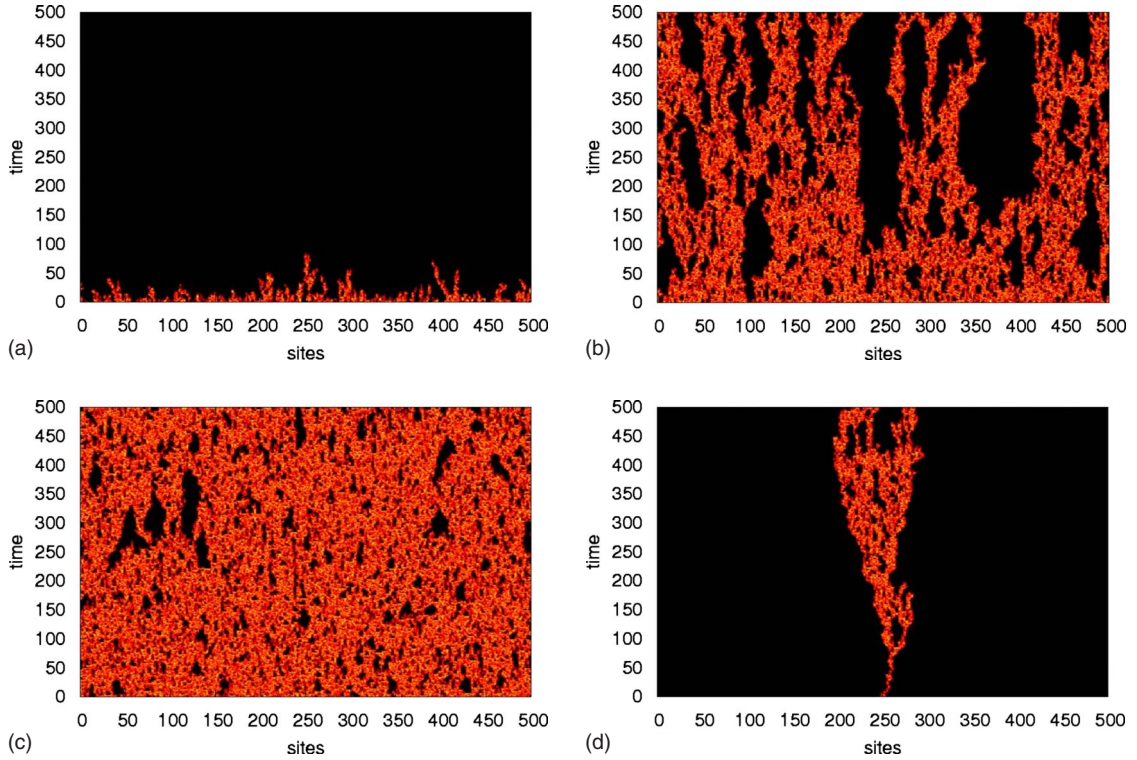


FIG. 4. (Color online) Space-time plot of CML for $\omega=0.068$, $L=500$, and $p=0.3$ for three different ϵ values. Laminar sites are dark in this representation. (a) $\epsilon=0.5$, where the turbulent spots vanish, implying a synchronous state. (b) $\epsilon=0.627$, where we clearly see the spatiotemporal intermittency regime. (c) $\epsilon=0.7$, where the system shows spatiotemporal chaos. (d) Spreading of three active seeds in an otherwise absorbing lattice of size $L=500$ at critical point $\epsilon_c=0.627$.

deed well portrays the role of the percolation probability. As DP is interpreted as a reaction-diffusion process which involves creation, coalescence, and death, we can consider stochastic time-dependent switching of coupling from repulsive to attractive as a dynamical analog to statistical process. So far coupled circle maps at certain parameter values studied by Janaki *et al.* [13] and Jabeen and Gupte [16] was the only known example of a coupled map lattice with a *unique* absorbing state whose transition falls in universality class of directed percolation. Here, we propose a coupled circle map lattice with coupling scheme incorporating the effects of creation, death, and coalescence as in general DP systems. We quantitatively discuss spatiotemporal intermittency obtained by stochastically coupled circle map lattice and its universality class. Numerical evidence suggests that such an analogy can be established from the estimates of the critical exponents for this CML.

The order parameter $m(\epsilon, L, t)$ is defined as the fraction of turbulent sites in the lattice averaged over many initial configurations. In the spatiotemporal chaos region, the density of turbulent sites decays and eventually saturates at some value. It is well known that for a continuous phase transition the saturation value of order parameter m_{sat} decays as a power law as the coupling strength ϵ approaches the critical value ϵ_c asymptotically. In addition, there are certain scaling exponents which we obtain as following the scaling relations as suggested by Hinrichsen [4]. We obtain the critical exponents for $p=0.3$, but the DP transition remains valid for all the points shown in the phase diagram in Fig. 2. Conventionally,

the exponent β is determined by measuring the stationary density of turbulent sites $m_{sat} \sim \Delta^\beta$, where $\Delta = |\epsilon - \epsilon_c|$, approaching the critical point ϵ_c from the side of spatiotemporal chaos. This estimate is inaccurate since the equilibration time to reach the saturated stationary value grows rapidly as the critical point is approached. This is called *critical slowing down*. The critical percolation threshold is obtained by measuring deviations from the asymptotic power-law decay,

$$m(t) \sim t^{-\delta}, \quad (4)$$

for a large system size. We start with initial conditions at which all sites are turbulent. In Fig. 5, three different values of coupling strength are shown for $p=0.3$. For $\epsilon=0.617$, the density of turbulent sites decays exponentially and the system reaches absorbing state. Critical coupling $\epsilon_c=0.627$ for $p=0.3$ shows an algebraic decay of order parameter with respect to time, which defines the critical exponent $\delta=0.159$ in agreement with DP. We take a system size of $L=5000$ which is large enough to neglect finite-size corrections, if any. Upon further increase in coupling strength, $\epsilon=0.636$, the fraction of turbulent sites saturates to a finite constant value. The order parameter scales with time and system size through the following scaling relation:

$$m(t, L, \epsilon_c) \simeq t^{\beta/\nu_\parallel} F(\Delta t^{1/\nu_\parallel}, t^{d/z}/L). \quad (5)$$

In Fig. 6(a), variations of order parameter for different distances from criticality are shown against the time. We plot $m(t)t^\delta$ vs $t(\epsilon - \epsilon_c)^{\nu_\parallel}$ for different deviations from criticality.

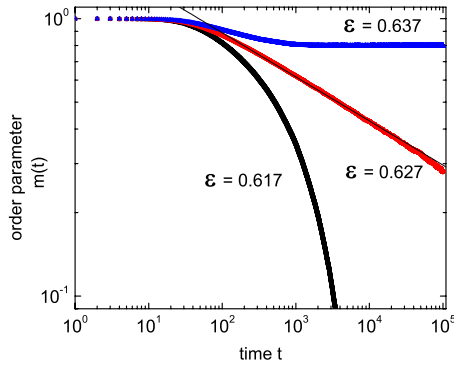


FIG. 5. (Color online) Log-log plot of order parameter $m(t)$ as a function of time for $p=0.3$ and $L=5000$ for three different ϵ values from bottom to top. (a) $\epsilon=0.617$, where the density of turbulent sites decays exponentially. (b) $\epsilon=0.627$, where order parameter decays as a power law with exponent $\delta=0.159$. (c) $\epsilon=0.637$, where the density saturates to a value. The line with a slope of 0.159 is plotted for reference.

The off-critical scaling is achieved at $\nu_{\parallel}=1.733$ at which all curves collapse as shown in Fig. 6(b). The exponent β can then be extracted from the relation $\beta=\delta\nu_{\parallel}$, whence $\beta=0.275$. The above procedure thus avoids the critical slowing down. The dynamic exponent z can be calculated using the finite-size scaling argument. Figure 7(a) shows a log-log (all logarithms are to the base 10) plot of order parameter $m(t)$ vs t for different lattice sizes $L=200, 250, 300, 350$ at the critical point ϵ_c . Figure 7(b) shows a double-logarithmic plot of $m(t)t^{\delta}$ vs t/L^z for various system sizes. The data collapse is obtained for dynamic exponent $z=1.58$. The dynamic exponent $z=\nu_{\parallel}/\nu_{\perp}$ gives a measure of how fast the local perturbation spreads. The exponent ν_{\parallel} is the spatial correlation exponent and ν_{\perp} is the temporal correlation exponent which can be obtained using the above relation, viz., $\nu_{\perp}=1.09$, in agreement with DP class.

IV. DYNAMIC SPREADING EXPONENTS

To further validate our conjecture that stochastic coupling can be considered as the dynamic analog of DP processes, we simulate the model presented in Eq. (1) starting with few turbulent (active) sites in an otherwise absorbing medium [33]. To counter strictly symmetric spreading [13], we start with three contiguous turbulent sites. The spreading phenomena can be seen in Fig. 4(d). In this type of simulations, the relevant variables are the number of active sites $N(t)$ averaged over all runs, the survival probability $P(t)$ averaged over many clusters, and the mean spreading distance (squared radius of gyration) from the origin of turbulent activity averaged over only surviving runs from the ensemble. At criticality, these quantities display asymptotic power law of the form

$$P(t) \sim t^{-\delta}, \quad N(t) \sim t^{\theta}, \quad R^2(t) \sim t^{z_s}, \quad (6)$$

with survival probability exponent δ , slip exponent θ , and spreading exponent z_s . All the dynamic simulations have

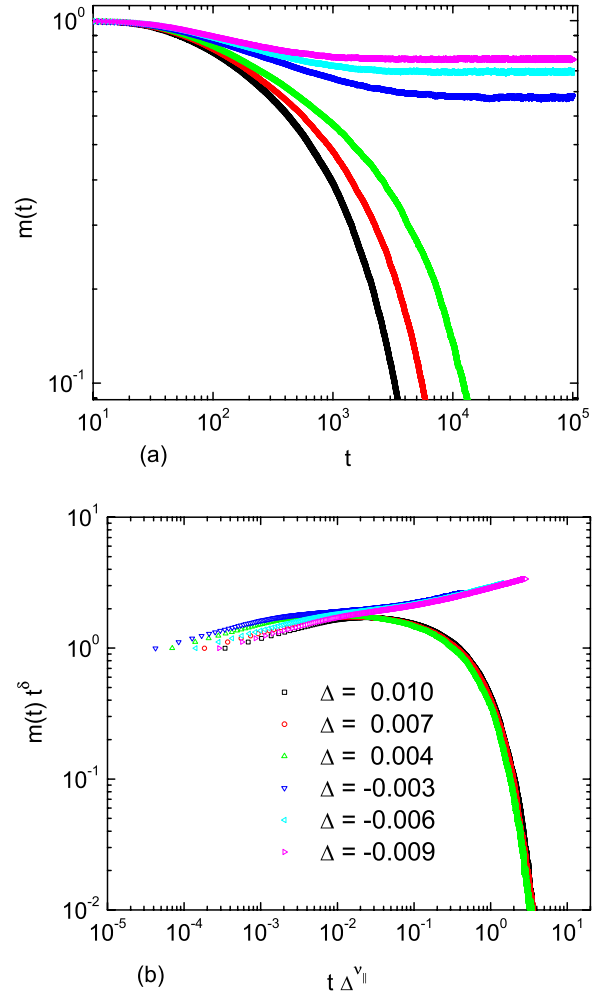


FIG. 6. (Color online) (a) Log-log plot of order parameter $m(t)$ as a function of time for $p=0.3$ and $L=5000$ for different values of $\epsilon=0.636, 0.633, 0.63, 0.623, 0.62, 0.617$ shown from top to bottom away from criticality. (b) The corresponding plot of data collapse according to scaling function (5) for different Δ . The data collapse is obtained for $\nu_{\parallel}=1.733$.

been performed for lattice size $L=5000$ and averaged over at least 5000 different configurations. We fix $p=0.3$ for the following simulations. Figure 8(a) shows the plot of survival probability $p(t)$ vs time t on a logarithmic scale in the inset for different ϵ . The power-law decay is obtained for critical coupling strength $\epsilon_c=0.627$ on a lattice size of 5000. The critical exponent associated with the survival probability was found to be $\delta=0.159+0.001$, in agreement with the corresponding DP exponent. This also shows that the *rapidity-reversal symmetry* pertaining to time invariance, which is obeyed in DP class, is followed in our model, too. This is owing to the fact that the exponents associated with critical density of turbulent sites $m(t)$ and survival probability $P(t)$ are the same. This means that such a time-reversal symmetry is possible in our model of CML with stochastic coupling. This adds credibility to the use of chaotic systems for studying stochastic processes. To estimate the critical exponent

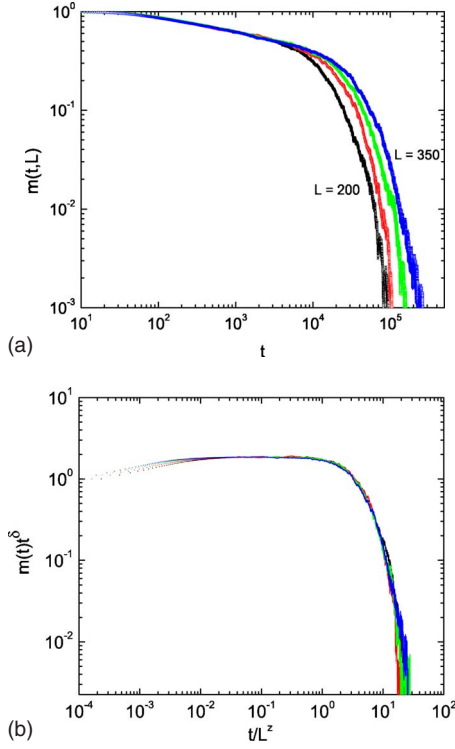


FIG. 7. (Color online) (a) Log-log plot of order parameter $m(t)$ as a function of time for $p=0.3$ and $\epsilon=0.627$ for different lattice size values $L=200, 250, 300, 350$. (b) Finite-size scaling for scaling function (5). This shows excellent data collapse with exponent $z=1.580$.

and transition points together, we determine the local slopes of the scaling variables. *Effective exponents* can be calculated by using the formula [34]

$$-\delta_t = \frac{\log_{10}[P(t)/P(t/b)]}{\log_{10} b}, \quad (7)$$

with $b=5$. At the critical point the value of exponent converges, whereas the off-critical curves have drastic curvatures, i.e., we can see that subcritical curves veer downward and supercritical curves deflect upward.

Figure 8(b) (inset) shows $N(t)$ vs t for supercritical ($\epsilon=0.637$), critical ($\epsilon_c=0.627$), and subcritical ($\epsilon=0.617$) regions. It can be seen that at criticality the number of turbulent sites $N(t)$ grows as a power law. Figure 8(b) shows the effective exponent $\theta(t)$.

The dynamic exponent z is related to z_s by the relation $z_s=2/z$. The effective exponent for mean-square spreading from the origin, z_s , is shown in Fig. 9. The radius of spreading increases algebraically as seen in the inset for ϵ_c .

V. CONCLUSIONS

In conclusion, we propose a model where negative and positive couplings are present in the lattice. We have studied the spatiotemporal properties of a lattice of coupled circle map whose coupling is switched between positive and negative with probability p . We explore the effect at each value of

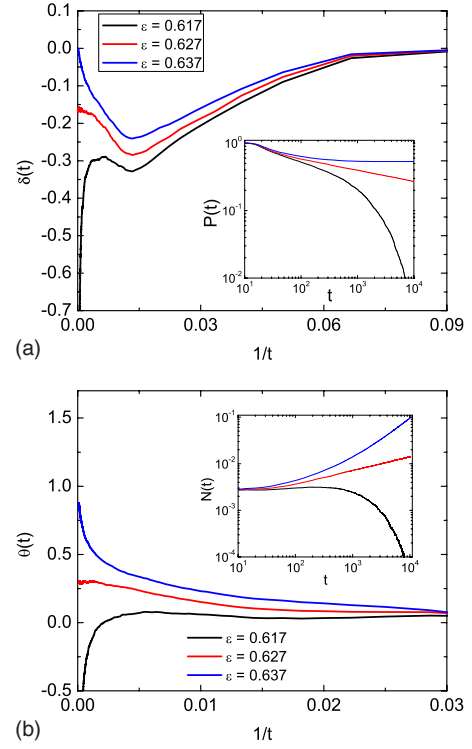


FIG. 8. (Color online) (a) Time-dependent behavior of effective exponent $\delta(t)$ for corresponding coupling strengths. Convergence is seen at $\delta \sim -0.159$ for ϵ_c . Survival probability $P(t)$ turbulent sites as a function of time for three different values of coupling strength $\epsilon=0.617, 627, 637$ shown in the inset. (b) Effective exponent $\theta(t)$ and average number of turbulent sites $\langle N(t) \rangle$ in the inset for same set of parameters.

p and try to investigate the impact of time-dependent switching of coupling. The time-dependent probabilistic switching of coupling has an interesting effect on spatiotemporal dynamics of the system. The first important implication is the stabilization of a local fixed point into a stable global attractor. We also provide evidence of continuous phase transition from a globally attracting spatiotemporal fixed point to spa-

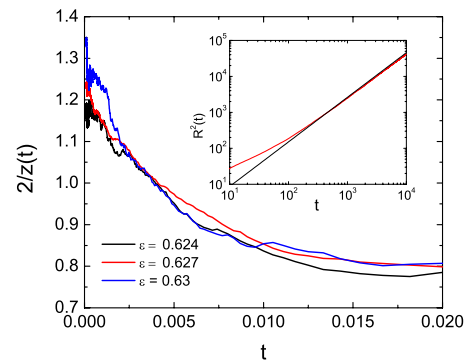


FIG. 9. (Color online) Time-dependent behavior of effective exponent $2/z$ for three different values of coupling strength $\epsilon=0.63, 0.627, 0.624$; coupling strengths from top to bottom. Convergence is seen at $2/z \sim 1.26$ for ϵ_c . Radius of mean-square spreading of active sites $\langle R^2(t) \rangle$ for critical coupling strength $\epsilon=0.627$ is shown in the inset.

TABLE I. Critical state exponents of the stochastically coupled circle map lattice. First row corresponds to critical coupling probability and critical coupling strength. The last row shows corresponding exponents of DP class.

p_c	ϵ_c	β	δ	ν_{\parallel}	ν_{\perp}	z	δ	θ	z_s
0.3	0.627	0.275	0.159	1.733	1.09	1.58	0.159	0.31	1.27
DP [4]		0.2764	0.1594	1.7338	1.096	1.5807	0.1594	0.3136	1.26

tiotemporal chaos with increasing coupling strength for most of the values of p . The implication of the stabilization of a fixed point is that it acts as a unique absorbing state. Studies on synchronization transition in locally coupled replicas of same systems suggest different universality classes for different synchronization transitions. The jump from one universality class DP to multiplicative noise (MN) occurs when chaos turns into stable chaos for a value of map parameter [35]. The random multiplier (RM) model of coupled piecewise linear maps is model where stochastic dynamics was considered. The transition in RM model belongs to DP class or MN class depending on values of propagation velocity of unsynchronized site clusters and transverse Lyapunov exponent [36]. The stochastic nature of dynamics was in terms of map parameters and deviations in replica system, but the nature of coupling was constant (democratic coupling).

The important motivation behind our model was to check whether one can mimic nonequilibrium stochastic processes by deterministic dynamical systems with addition of an element of randomness equivalent to percolation probability. The numerical results suggest a strong evidence that the dynamic phase transition from a spatiotemporal fixed point to spatiotemporal chaos, via spatiotemporal intermittency, is in class of directed percolation. Several spreading and non-spreading exponents obtained are shown in Table I. The earlier studies of positively couple circle map showed that the onset of spatiotemporal intermittency is in DP class at some specific parameter values of circle map. Here, we find that

for most of the values of coupling probability p , there is a critical coupling strength ϵ at which the transition occurs. This continuum of behavior between two extreme situations ($p=0$ and 1) makes one understand the fact that the reaction-diffusion mechanism in stochastic process can be successfully recovered by a suitable model of dynamical processes. Thus, it may be deduced that the creation, coalescence, and death processes in DP can be considered analogous to attractive and repulsive couplings in CMLs. It is important to note that our model follows the Grassberger conjecture applicable to DP systems. The stochastic coupling is a short-range process as it involves only nearest neighbor, without any additional symmetries or quenched randomness. A possible extension of this problem is to obtain a partial differential equation for stochastically coupled circle maps and try to find elements of DP-Langevin equation, thus establishing analytical congruency on the lines of [37]. We hope to examine the possibility in our future work.

ACKNOWLEDGMENTS

I wish to thank M. A. Saif and P. M. Gade for valuable discussions. I also thank Sudeshna Sinha and anonymous referees for important suggestions improving earlier versions of the paper. I am grateful to R. K. Pathak for critical reading of the manuscript. I acknowledge C.S.I.R, India for financial support.

-
- [1] T. Vojta, *Phys. Rev. E* **55**, 5157 (1997).
 - [2] R. M. Ziff, E. Gulari, and Y. Barshad, *Phys. Rev. Lett.* **56**, 2553 (1986).
 - [3] G. Odor, *Rev. Mod. Phys.* **76**, 663 (2004).
 - [4] H. Hinrichsen, *Adv. Phys.* **49**, 815 (2000).
 - [5] V. Ahlers and A. Pikovsky, *Phys. Rev. Lett.* **88**, 254101 (2002).
 - [6] F. Ginelli, V. Ahlers, R. Livi, D. Mukamel, A. Pikovsky, A. Politi, and A. Torcini, *Phys. Rev. E* **68**, 065102(R) (2003).
 - [7] R. Dickman, M. A. Munoz, A. Vespignani, and S. Zapperi, *Braz. J. Phys.* **30**, 27 (2000).
 - [8] K. A. Takeuchi, M. Kuroda, H. Chate, and M. Sano, *Phys. Rev. Lett.* **99**, 234503 (2007).
 - [9] S. N. Dorogovtsev, A. V. Goltsev, and J. F. F. Mendes, *Rev. Mod. Phys.* **80**, 1275 (2008).
 - [10] H. Chate and P. Manneville, *Physica D* **32**, 409 (1988).
 - [11] P. Grassberger and T. Schreiber, *Physica D* **50**, 177 (1991).
 - [12] J. Rolf, T. Bohr, and M. H. Jensen, *Phys. Rev. E* **57**, R2503 (1998).
 - [13] T. M. Janaki, Sudeshna Sinha, and N. Gupte, *Phys. Rev. E* **67**, 056218 (2003).
 - [14] G. I. Menon, Sudeshna Sinha, and P. Ray, *EPL* **61**, 27 (2003).
 - [15] Y. Pomeau, *Physica D* **23**, 3 (1986).
 - [16] Z. Jabeen and N. Gupte, *Phys. Rev. E* **74**, 016210 (2006).
 - [17] M. Das, B. Chakrabarti, C. Dasgupta, S. Ramaswamy, and A. K. Sood, *Phys. Rev. E* **71**, 021707 (2005).
 - [18] Z. Jabeen and Sudeshna Sinha, *Phys. Rev. E* **78**, 066120 (2008).
 - [19] L. S. Tsimring, N. F. Rulkov, M. L. Larsen, and M. Gabbay, *Phys. Rev. Lett.* **95**, 014101 (2005).
 - [20] Z. Qu, Y. Shiferaw, and J. N. Weiss, *Phys. Rev. E* **75**, 011927 (2007).
 - [21] Z. Neufeld and T. Vicsek, *J. Phys. A* **28**, 5257 (1995).
 - [22] X. Chen and J. E. Cohen, *J. Theor. Biol.* **212**, 223 (2001).
 - [23] C. van Vreeswijk and H. Sompolinsky, *Science* **274**, 1724 (1996).
 - [24] Y. Chen, J. Xiao, W. Liu, L. Li, and Y. Yang, *Phys. Rev. E* **80**, 046206 (2009).

- [25] P. M. Gade, D. V. Senthilkumar, Sukratu Barve, and Sudeshna Sinha, *Phys. Rev. E* **75**, 066208 (2007).
- [26] D. Zanette and A. Mikhailov, *Physica D* **194**, 203 (2004).
- [27] Sudeshna Sinha, *Phys. Rev. E* **66**, 016209 (2002).
- [28] M. P. K. Jampa, A. R. Sonawane, P. M. Gade, and S. Sinha, *Phys. Rev. E* **75**, 026215 (2007).
- [29] A. Mondal, Sudeshna Sinha, and J. Kurths, *Phys. Rev. E* **78**, 066209 (2008).
- [30] F. M. Atay, J. Jost, and A. Wende, *Phys. Rev. Lett.* **92**, 144101 (2004).
- [31] C. Masoller and A. C. Marti, *Phys. Rev. Lett.* **94**, 134102 (2005).
- [32] T. Turova, *BioSystems* **40**, 197 (1997).
- [33] P. Grassberger and A. de la Torre, *Ann. Phys. (N.Y.)* **122**, 373 (1979).
- [34] P. Grassberger, *J. Phys. A: Math. Gen.* **22**, 3815 (1989).
- [35] F. Bagnoli and R. Rechtman, *Phys. Rev. E* **73**, 026202 (2006).
- [36] F. Ginelli, R. Livi, A. Politi, and A. Torcini, *Phys. Rev. E* **67**, 046217 (2003).
- [37] E. Katzav and L. F. Cugliandolo, *Physica A* **371**, 96 (2006).